



# Myomesin is a Molecular Spring with Adaptable Elasticity

Roman Schoenauer<sup>1†</sup>, Patricia Bertoncini<sup>2†</sup>, Gia Machaidze<sup>3</sup>, Ueli Aebi<sup>3</sup>  
Jean-Claude Perriard<sup>1\*</sup>, Martin Hegner<sup>2\*</sup> and Irina Agarkova<sup>1</sup>

<sup>1</sup>*Institute of Cell Biology  
ETH Zürich-Hönggerberg  
CH-8093 Zürich, Switzerland*

<sup>2</sup>*Institute of Physics, University  
of Basel, CH-4056 Basel  
Switzerland*

<sup>3</sup>*M.E. Müller Institute for  
Structural Biology, Biozentrum  
University of Basel, 4056 Basel  
Switzerland*

The M-band is a transverse structure in the center of the sarcomere, which is thought to stabilize the thick filament lattice. It was shown recently that the constitutive vertebrate M-band component myomesin can form antiparallel dimers, which might cross-link the neighboring thick filaments. Myomesin consists mainly of immunoglobulin-like (Ig) and fibronectin type III (Fn) domains, while several muscle types express the EH-myomesin splice isoform, generated by the inclusion of the unique EH-segment of about 100 amino acid residues (aa) in the center of the molecule. Here we use atomic force microscopy (AFM), transmission electron microscopy (TEM) and circular dichroism (CD) spectroscopy for the biophysical characterization of myomesin. The AFM identifies the “mechanical fingerprints” of the modules constituting the myomesin molecule. Stretching of homomeric polyproteins, constructed of Ig and Fn domains of human myomesin, produces a typical saw-tooth pattern in the force-extension curve. The domains readily refold after relaxation. In contrast, stretching of a heterogeneous polyprotein, containing several repeats of the My6-EH fragment reveals a long initial plateau corresponding to the sum of EH-segment contour lengths, followed by several My6 unfolding peaks. According to this, the EH-segment is characterized as an entropic chain with a persistence length of about 0.3 nm. In TEM pictures, the EH-domain appears as a gap in the molecule, indicating a random coil conformation similar to the PEVK region of titin. CD spectroscopy measurements support this result, demonstrating a mostly non-folded conformation for the EH-segment. We suggest that similarly to titin, myomesin is a molecular spring, whose elasticity is modulated by alternative splicing. The Ig and Fn domains might function as reversible “shock absorbers” by sequential unfolding in the case of extremely high or long sustained stretching forces. These complex visco-elastic properties of myomesin might be crucial for the stability of the sarcomere.

© 2005 Elsevier Ltd. All rights reserved.

**Keywords:** striated muscle; M-band; myomesin; titin; atomic force microscopy

\*Corresponding authors

## Introduction

Vertebrate striated muscle sarcomeres contain in addition to thick and thin filaments a complex network of cytoskeletal proteins. These proteins form two transverse structures, which are essential

for the regular arrangement of the contractile filaments: the Z-disc, which anchors the actin filaments and the M-band, which is thought to cross-link the myosin filaments. The elastic connection between them is provided by titin,<sup>1</sup> which spans from the Z-disc (N terminus) to the M-band (C terminus).<sup>2</sup> Titin is tightly bound to the thick filaments in the A-band, while its I-band portion, consisting of serially connected immunoglobulin (Ig)-domain chains and unique PEVK and N2B regions, is extensible. The molecular basis for the elasticity of titin is quite well understood due to the recent progress in single-molecule analysis

† R.S. & P.B. contributed equally to this work.

Abbreviations used: TEM, transmission electron microscopy; CD, circular dichroism; Ig, immunoglobulin-like; Fn, fibronectin-like; AFM, atomic force microscopy.

E-mail address of the corresponding authors:

jcp@cell.biol.ethz.ch; martin.hegner@unibas.ch

techniques such as optical tweezers and atomic force microscopy (AFM).<sup>3,4</sup> There are two main sources of elasticity in the extensible I-band portion of this protein: one deriving from the straightening of the Ig domains chain, the other from the extension of the largely non-folded PEVK and N2B regions.<sup>5</sup> Upon stretching sarcomeres, first the Ig segments straighten while their individual Ig domains remain folded. When the sarcomeres are further stretched (beyond 2.7  $\mu\text{m}$ ), the PEVK extension becomes dominant.<sup>6</sup> Recent analyses revealed that the unique PEVK region not only acts as an entropic spring, but also has actin-binding properties and was therefore suggested to produce a viscous force component opposing filament sliding.<sup>7</sup> Strong stretches exhaust the elasticity of the titin molecule and lead to the sequential unfolding of the modular domains.<sup>5</sup> Single-molecule manipulations by AFM of recombinant fragments of titin have shown a characteristic saw-tooth pattern in the force-extension relationship, with each peak corresponding to the unfolding of a single domain.<sup>8</sup> The unfolding force of individual Ig domains ranged from 150 pN to 300 pN and the modules readily refold upon release of tension.<sup>8</sup> Ig domains located in different portions of the extensible part of I-band titin demonstrate a hierarchy of mechanical stability, with the weakest Ig-domains (unfolding force  $\sim$ 150 pN) located adjacent to the Z-disc.<sup>9</sup> The differentially expressed domains in the central portion of I-band titin show intermediate stability ( $\sim$ 180 pN), while the mostly stable domains ( $\sim$ 220 pN) constitute the distal portion of the titin I-band region, near the tip of the thick filament.<sup>10</sup> Further investigations revealed that the fibronectin (Fn) domains have in general lower unfolding forces (100–200 pN) than the Ig domains (150–300 pN).<sup>11,12</sup> It has been discussed that some parts of titin may participate in accommodating changes in sarcomere length through reversible unfolding and refolding.<sup>13</sup> Thus, single-molecule measurements of the individual titin domains allowed reconstruction of the mechanical characteristics of the whole molecule<sup>9</sup> and the clarification of the mechanical function of titin in the sarcomere.<sup>3,4</sup>

The sliding filament model of muscle contraction implies that the central position of the thick filament in the sarcomere is intrinsically unstable in the working sarcomere. Due to differences in the number or extent of cross-bridge activations or due to slight variations in the overlap with actin filaments, the forces generated on two halves of activated thick filaments cannot be identical. Any initial imbalance of forces will be further enhanced during contraction due to the progressive displacement of thick filaments from the center. The A-bands, moved towards one of the Z-discs, were indeed observed in electron microscope (EM) pictures of activated skeletal muscle.<sup>14,15</sup> However, the stability of sarcomeric contraction requires the proper centering of the thick filaments at the end of each contraction cycle. It is believed that elastic titin

filaments, connecting the thick filaments with the Z-discs, accomplish this important job.<sup>16–18</sup> However, as suggested recently, an important contribution comes from the M-band bridges, cross-linking the thick filaments.<sup>19</sup> Due to this connection the random initial imbalance of the cross-bridge forces gets averaged through all thick filaments present in one sarcomere; this significantly facilitates the efforts of titin to restore the status quo. This model implies that the M-band filaments are stretched during the contraction cycle, due to force differences between neighboring thick filaments (Figure 1(a)). Unfortunately, no information is presently available on the mechanical properties of structural M-band proteins at the molecular level.

The main candidates for the role of M-bridges, connecting the myosin filaments in the M-band<sup>20</sup> are two closely related proteins of the Ig-superfamily, myomesin and M-protein.<sup>21</sup> These are modular proteins, consisting of a unique N-terminal domain followed by a conserved sequence of 12 immunoglobulin-like (Ig) and fibronectin type III (Fn) domains<sup>22,23</sup> (Figure 1(b)). In contrast to M-protein, which has a muscle-type specific expression pattern,<sup>24</sup> myomesin is expressed in all types of vertebrate striated muscles<sup>25</sup> and localizes to the nascent M-band already in the first sarcomeres in embryonic heart.<sup>26</sup> Although a proof for the essential function of myomesin awaits the generation of a knockout model, it is interesting that mice with a conditional knockout for the M-band region of titin (including the myomesin binding site) show signs of muscle weakness and progressive sarcomere disassembly.<sup>27</sup> The N terminus of myomesin is involved in the interaction with myosin,<sup>28–30</sup> the central part interacts with the titin m4 domain<sup>29</sup> and muscle-type creatine kinase (MM-CK)<sup>31</sup> while the C-terminal domain 13 of myomesin was recently shown to form antiparallel dimers.<sup>32</sup> In the central part of the molecule an alternative splicing event can take place<sup>25,33</sup> leading to the insertion of the additional EH-segment (96 aa in the human sequence) between domains My6 and My7 (Figure 1(b)). This generates the EH-isoform, which is the main myomesin species in the embryonic heart of all higher vertebrates<sup>25</sup> and shows a fiber-type dependent expression pattern in adult mouse skeletal muscle.<sup>34</sup> Interestingly, this unique EH-segment is rather heterogeneous in sequence between different species<sup>25</sup> and seems to be in an intrinsically disordered state according to computer simulations (Predictors of Natural Disordered Regions, PONDR). The recently published three-dimensional model of the M-band<sup>32</sup> suggests that antiparallel dimers of myomesin cross-link myosin filaments in a similar way as  $\alpha$ -actinin cross-links actin filaments in the Z-disc. Therefore, the myomesin molecule may be stretched during sarcomere contraction due to small deviations of neighboring thick filaments.<sup>19</sup>

To characterize the mechanical properties of

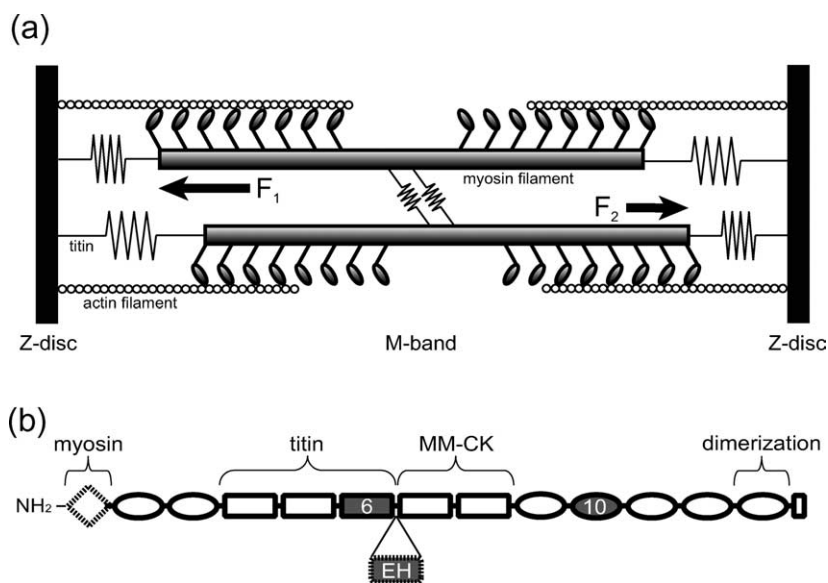


**Figure 1.** (a) Schematic representation, demonstrating the role of the M-band in the contracting sarcomere. The cross-bridge forces acting on both halves ( $F_1$ ,  $F_2$ ) are not equal, leading to progressive deviations of the thick filaments from the center during contraction. This is partially compensated by the M-band filaments, which equilibrate these force imbalances over all thick filaments present in one sarcomere. Adapted from Agarkova *et al.*<sup>19</sup> (b) Schematic representation of myomesin. Myomesin is mainly composed of immunoglobulin-like (ellipses) and fibronectin type III domains (rectangles). The EH-isoform has an additional EH-segment (EH, in grey) inserted in the center of the molecule. EH-segment as well as

N-terminal domain My1 are predicted to be in an intrinsically disordered conformation (shown by broken lines). Myomesin domain My1 interacts with myosin, My4-6 is the titin-binding region, My7-8 interacts with MM-CK and My13 mediates an antiparallel dimerization. In addition to the EH-segment, domains My6 (6, in grey) and My10 (10, in grey) have been selected for the cloning of polyproteins.

myomesin and to elucidate its function in the M-band, we performed single-molecule measurements on different myomesin domains. The stretching of homomeric polyproteins, constructed of My6 (Fn) or My10 (Ig) domains of human myomesin by AFM gives rise to a characteristic saw-tooth pattern in the force-extension curve. In contrast, the stretching of a heterogeneous polyprotein (several repeats of My6-EH) reveals a saw-tooth pattern only after a long initial plateau corresponding to the sum of the contour lengths of the stretched EH-segments. Transmission EM (TEM) pictures and CD measurements show that this domain is present in a mostly non-folded state comparable to the PEVK domain of titin.<sup>35</sup> Thus the EH-segment might function similarly to the PEVK segment of titin and may produce a restoring force by a mechanism of entropic elasticity. Our results suggest that myomesin is a molecular spring in the M-band of the sarcomere, whose elastic properties are modified by alternative splicing.

## Results

### CD-spectrum of recombinant human EH-segment reveals the absence of a defined secondary structure

In order to study the structural properties of the alternatively spliced EH-segment of human myomesin, we measured the CD-spectrum of this domain (Figure 2). The spectrum contains one strong minimum at 199 nm and a negative shoulder at ~215 nm, which corresponds to a mostly non-

folded protein chain with residual secondary structure.<sup>36</sup> This result strongly supports the hypothesis, based on computer predictions (PONDR), that the EH-segment has no defined secondary structure and is present in a mostly non-folded state at physiological condition. In contrast, CD spectroscopy measurements of the full-length myomesin molecule lacking the EH-segment<sup>28</sup> show a beta-sheet spectrum typical for Ig domains (minimum at ~210 nm), which can be explained by the dominant presence of this type of secondary structure in the whole protein.

### The EH-segment appears less compact as the Fn domains in molecules visualized in TEM

The molecular anatomy of recombinant myomesin constructs was visualized by TEM to confirm the non-folded conformation of the EH-segment by glycerol spraying/rotary shadowing of myomesin polyproteins (Figure 3). Both, (My10)<sub>9</sub> (Figure 3(a)) and (My6)<sub>8</sub> (Figure 3(b)) polyproteins appear as randomly bent rod-like structures. In contrast, the micrographs of the (My6-EH)<sub>4</sub> polyproteins (Figure 3(c)) show groups of four globular domains, evidently linked by an “invisible thread” and spaced evenly. Some molecules seem to be fragmented and contain fewer than four beads. We interpret these results as evidence of four tightly folded My6 domains giving rise to the bead-like structures separated by three EH-segments, which are not visible after rotary shadowing. Considering that the Fn domains are connected by 116 aa comprising the EH-segment and the linkers, this region has a contour length of 34.8 nm (0.3 nm/aa × 116 aa). However, the observed end-to-end length

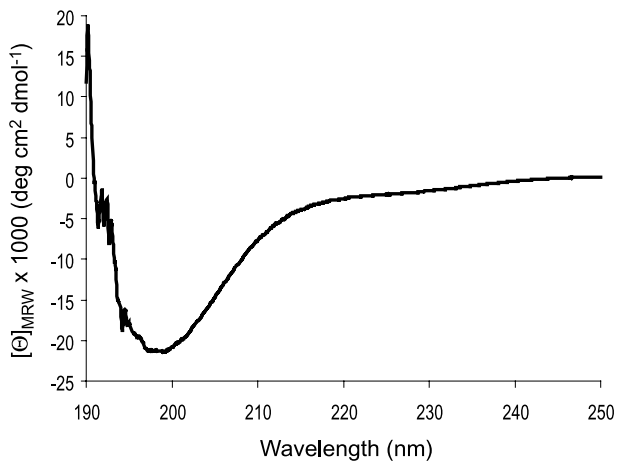


**Figure 2.** Circular dichroism spectrum of the human EH-segment. Note the strong minimum at 199 nm and a negative shoulder at  $\sim 215$  nm, which corresponds to a mostly unstructured protein with no defined secondary structure. ( $\Theta_{\text{MRW}}$ ) is the mean molar ellipticity.

of the EH-domain is much smaller than its contour length, suggesting that this region is coiled in the relaxed state. The invisibility of the EH-segment in EM micrographs indicates that it forms a much less compact structure than the folded My6 domain and cannot be visualized by rotary shadowing. The difference between the appearance of My6 or My10 and the My6-EH polyproteins supports the view that the EH-region is largely a non-folded polypeptide also in the native state.

### The mechanical stability of My6 and My10

In order to measure the mechanical properties of individual myomesin domains, we used atomic

force microscopy. This technique was designed specifically to study the force-extension characteristics of single molecules with high precision. First, we constructed homomeric polyproteins containing repeats of myomesin domains My6 (Fn) or My10 (Ig). Stretching such modular proteins normally results in the subsequent unfolding of the globular domains. Because the exact three-dimensional structures of My6 and My10 are not identified yet, we determined their boundaries by comparison to the known X-ray structure of similar domains (see Materials and Methods).

The stretching of (My6)<sub>8</sub> polyproteins at a pulling speed of 1000 nm/s results in force-extension curves with the expected saw-tooth patterns (Figure 4(a)) revealing unfolding forces of around 190 pN ( $190(\pm 41)$  pN,  $n=299$ ; Figure 4(b)). This value is comparable to the already published data of Fn domains of titin (A-band titin, 180 pN; I-band titin, 200 pN<sup>11</sup>) and fibronectin (75–220 pN<sup>37</sup>). A fit of the worm-like chain (WLC) model of polymer elasticity<sup>38</sup> to the force extension curve of (My6)<sub>8</sub> (Figure 4(a), broken line and dotted lines) shows an increase in contour length of  $\sim 26.3$  nm per force peak, which is consistent with the length of an unfolded domain calculated as the predicted number of amino acid residues between the first and last  $\beta$ -sheet ( $88 \text{ aa} \times 0.3 \text{ nm/aa} = 26.4 \text{ nm}$ ).

If the height of each individual force-peak is plotted as a function of its position in the saw-tooth pattern, a hierarchical relationship is observed. There is a tendency for the domains unfolded first to have slightly lower unfolding forces than the subsequent domains, which can be predicted from theoretical studies.<sup>39</sup> An average increase in force of 7.4 pN (Figure 4(c)) was determined from one peak to the next, which may result from the decrease in unfolding probability, as more domains are

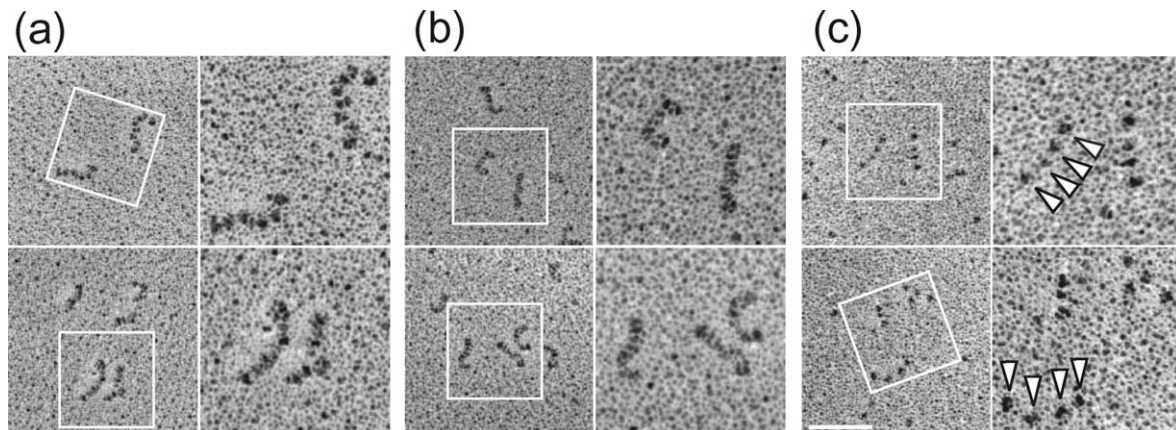


**Figure 3.** TEM images of individual myomesin polyproteins. (My10)<sub>9</sub> (a), (My6)<sub>8</sub> (b), and (My6-EH)<sub>4</sub> (c) molecules as seen after glycerol spraying/rotary metal shadowing. The right panels in (a)–(c) represent twofold magnifications of the squares framed in the left panels. The (My10)<sub>9</sub> and (My6)<sub>8</sub> polyproteins are visible as randomly bent rod-like structures. The (My10)<sub>9</sub> molecules appear longer and slightly less compact than the (My6)<sub>8</sub> ones, which can be explained by the higher number of modules and by the longer linker length in the (My10)<sub>9</sub> polyprotein (35 aa) compared to (My6)<sub>8</sub> (15 aa). In contrast, rotary metal-shadowed images of the (My6-EH)<sub>4</sub> construct reveal the My6 modules as four small globules (arrowheads), evidently connected by an “invisible thread” (i.e. the EH-segment). The scale bar represents 20 nm and applies to the left panels of (a), (b) and (c).

unfolded. Because the AFM tip picks up the molecule at random locations in the polyproteins, the number of peaks observed serves as a count of the number of modules contained in the segment that was picked up. The linker extension of a polyprotein can be determined by fitting the WLC model to the initial part of the force-extension curve, before any unfolding is observed ( $L_0$ , broken line; Figure 4(a)). It depends on the number of modules picked up by the AFM tip and represents the length of the fully stretched chain before any unfolding occurs. A plot of  $L_0$  versus the number of My6 modules shows a slope of 3.7 nm/module, which is close to the predicted linker length (15 aa  $\times$  0.3 nm/aa = 4.5 nm; Figure 4(d)).

To compare the mechanical characteristics of the Fn and Ig domains of myomesin, we constructed a

second homomeric polyprotein consisting of a sequence of several Ig domains My10. Figure 5(a) shows a force-extension curve obtained from the (My10)<sub>9</sub> polyprotein including the fit of the WLC model (broken line and dotted lines). The average unfolding force of the My10 domain is  $\sim$ 200 pN ( $203(\pm 50)$  pN) at a pulling speed of 1000 nm/s. This value is slightly higher compared to the My6 (Fn) domain, but the difference is not significant. The contour length of (My10)<sub>9</sub> is higher ( $\sim$ 27.9 nm per domain), corresponding to the bigger predicted length of an unfolded My10 domain (95 aa) compared to the My6 domain (88 aa). The initial peaks shown stem from short-range unspecific interactions, whereas the first peak used for fitting exhibits the right length ( $L_0$ , broken line) for an individual My10 polyprotein being present within

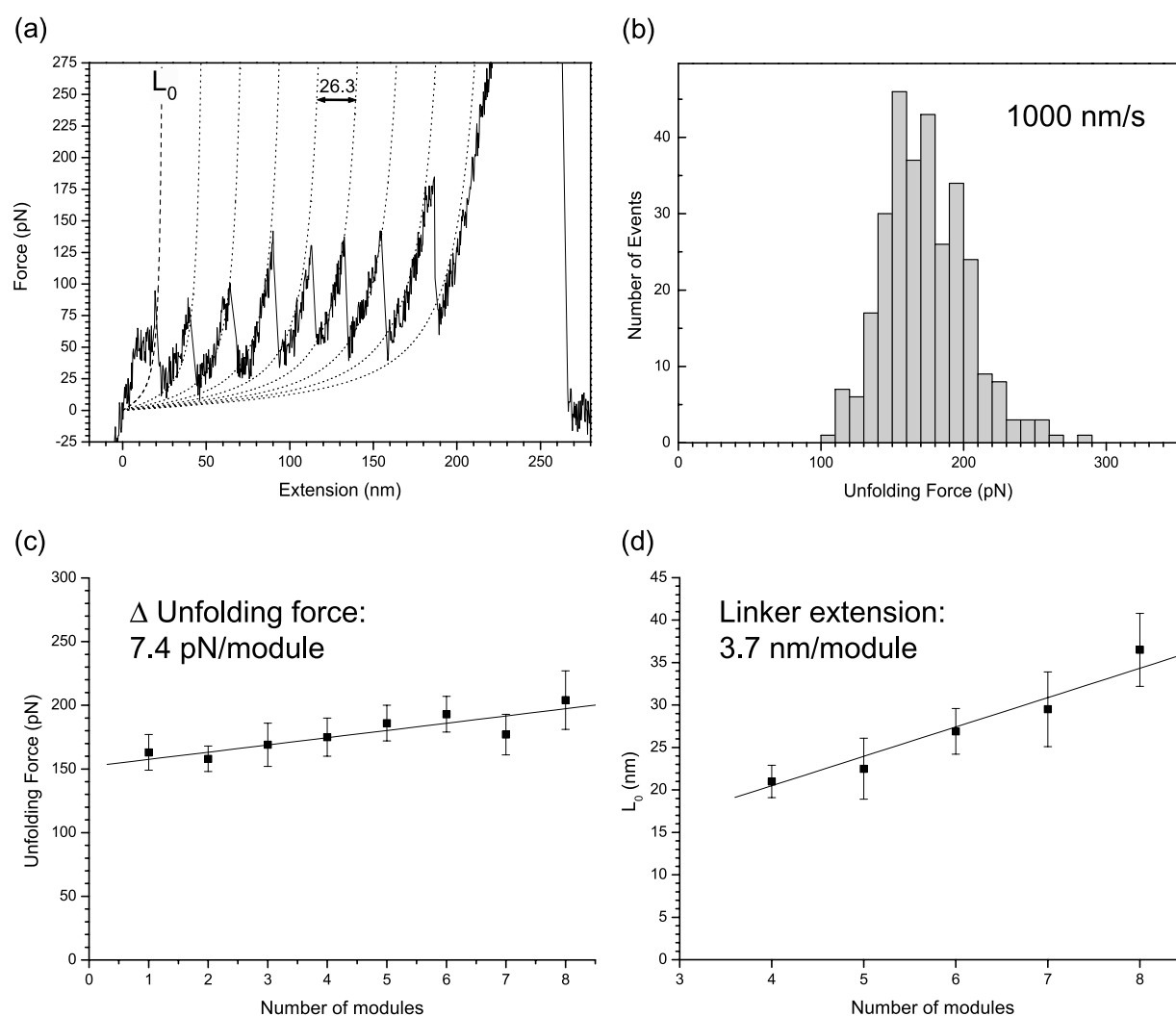


**Figure 4.** The mechanical properties of myomesin domain My6 (Fn). (a) Stretching of (My6)<sub>8</sub> polyproteins at a pulling speed of 1000 nm/s results in force-extension curves with the typical saw-tooth pattern. The curves show an increase in contour length of  $26.3(\pm 1.3)$  nm per unfolded domain. The broken line ( $L_0$ , linker extension) and the dotted lines show a fit of the WLC model of polymer elasticity. (b) Probability distribution of the unfolding force of My6 revealing a mean value of  $190(\pm 41)$  pN ( $n=299$ ) with a pulling speed of 1000 nm/s. (c) Relationship between the unfolding force and the force-peak position in the saw-tooth pattern obtained from (My6)<sub>8</sub> polyproteins. The slope of the line corresponds to an increase of 7.4 pN/peak. (d) The linker extension  $L_0$  also shows a linear dependence on the number of modules picked up by the AFM tip with a slope of 3.7 nm/module. The error bars in (c) and (d) correspond to the standard deviation.

the tip and the substrate interface. These measurements suggest that the mechanical stability of domain My10 is rather similar to the Ig segments of the differentially spliced (I65-70) regions of titin but significantly lower than that of the constitutive (I91-98) regions.<sup>10</sup> Furthermore, the Ig domain I27 of titin shows comparable characteristics (unfolding force  $\sim 200$  pN, extension of contour length: 28.1 nm/module (89 aa)).<sup>40</sup>

### The rate dependency of mechanical unfolding

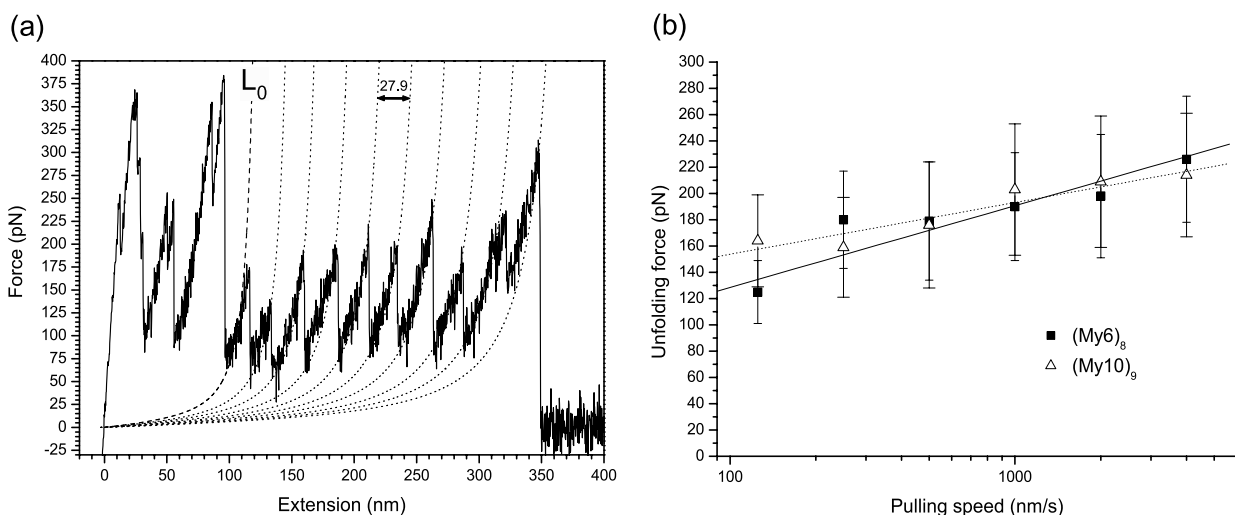
During muscle contraction, the domains of structural muscle proteins such as titin and myomesin may be stretched with a wide range of speeds. Since the mechanical characteristics may not be the same at different pulling speeds, as shown for titin,<sup>11,40</sup> we also studied the rate-dependency of the stability of myomesin domains.

Figure 5(b) shows the dependence of the unfolding forces of myomesin domains My6 (Fn) and My10 (Ig) on the pulling speed. For both domains, the average unfolding force shows a linear dependency with the logarithm of the pulling speed. With an increase of pulling speed from 125 nm/s to 4000 nm/s, the unfolding force of My6 rises from 125 pN to 226 pN, whereas My10 shows values from 164 pN to 214 pN. These data are similar to the already published unfolding forces of titin Ig and Fn domains.<sup>11</sup> Although the unfolding force of domain My10 shows a slightly weaker dependence on the pulling speed compared to My6, the difference is not significant. For My10, the unfolding kinetics are strikingly similar to the differentially spliced (I65-70) Ig segment of titin.<sup>10</sup>

Furthermore, the mechanical properties of My6 are comparable to individual Fn domains of fibronectin.<sup>37</sup>

### Myomesin domains can refold again after unfolding

Titin Ig domains are believed to fold spontaneously<sup>41</sup> and it is speculated that reversible folding may play a physiological role under over-stretch conditions.<sup>42</sup> In order to test if myomesin domains also are able to refold after mechanical unfolding, we used a two-pulse stretching protocol to repeatedly stretch and relax a single protein. Subsequent extension traces of the same molecule were recorded and after each extension, the polyprotein was allowed to relax completely and remained attached to the AFM tip (up to 20 cycles). After a variable relaxing time (1.5, 5 or 10 s) the protein was stretched again and the number of force peaks was counted. The number of extended domains was typically less than the maximum since the polyprotein is picked at a random length and the total extension of the protein is limited by detachment. Statistical analysis for the My6 (Fn) domain shows a refolding rate of 74% (1.5 s relaxing time), 85% (5 s) and 100% (10 s), which is comparable to the Fn domains of fibronectin.<sup>37</sup> These data reveal that most of the unfolded My6 domains refold spontaneously upon relaxation and that the refolding rate is dependent on the relaxing time. In addition, domain My10 (Ig) also has the ability to refold after mechanical unfolding with a refolding rate of  $\sim 50\%$  (relaxing time, 1.5 s). These results show that a big fraction of myomesin domains



**Figure 5.** The mechanical stability of myomesin domain My10 (Ig). (a) Stretching of  $(\text{My}10)_9$  polyproteins at a pulling speed of 1000 nm/s results in force-extension curves showing a mean unfolding force of  $203(\pm 50)$  pN and an increase in contour length of  $27.9(\pm 1.5)$  nm per unfolded domain. After an initial unspecific interaction, possibly due to a second molecule adhering to the tip or due to short-range interactions, the individual My10 (Ig) domains are unfolded unit by unit. The broken line ( $L_0$ , linker extension) and the dotted lines show the fit of the WLC model. (b) Comparison of velocity dependence of the mean unfolding force on the pulling speed for the My6 (Fn, black squares) and My10 (Ig, white triangles) domains of myomesin. The unfolding kinetics of both domains are very similar and show the typical linear dependence on the logarithm of the pulling speed (lines correspond to linear fit). The error bars correspond to the standard deviation. Pulling speed, 125–4000 nm/s.

refolds in less than 1.5 seconds if the protein is fully relaxed. The observation that myomesin domains can be unfolded in a reversible manner raises the possibility that this mechanism is of physiological importance in case of extremely high or extremely long-lasting stretching forces.

### Elasticity measurements of the EH-segment

We further used the AFM technique to investigate the mechanical properties of the EH-segment of myomesin. Although it seems obvious to engineer a polyEH protein for single-molecule AFM, stretching a random coil would give a featureless force-extension curve that would be difficult to distinguish from that observed for a denatured protein fragment. Hence, we used the My6 module, whose molecular "fingerprint" was identified in the previous experiment, as an easily recognizable marker for the boundaries of the EH-segment. Figure 6(a) shows several force-extension curves

for the  $(\text{My6-EH})_4$  polyprotein at a pulling speed of 500 nm/s. The characteristic fingerprint of the integrated My6 module shows that it unfolds at around 180 pN, extending the contour length of the protein by 26.3 nm. Four types of recordings are shown with one (curve 1), two (curves 2 and 4), three (curve 3), and four (curve 5) My6 unfolding events, excluding the last peak (detachment of the molecule from the AFM tip). In contrast to the My6 polyproteins, the stretching of a  $(\text{My6-EH})_4$  polyprotein produces a saw-tooth pattern only after an initial spacer  $L_0$ , ranging from  $\sim 20$  nm to  $\sim 120$  nm, corresponding to the stretching of one (curve 1), two (curves 2 and 3), or three (curves 4 and 5) EH-segments. Because the polyprotein is constructed of alternating My6 and EH domains, if four (three) My6 unfolding peaks are observed, at least three (two) EH-segments must have been stretched. If we observe two My6 unfolding peaks, at least one EH-segment has been extended. In this way we can be sure that the EH-segments are stretched and that

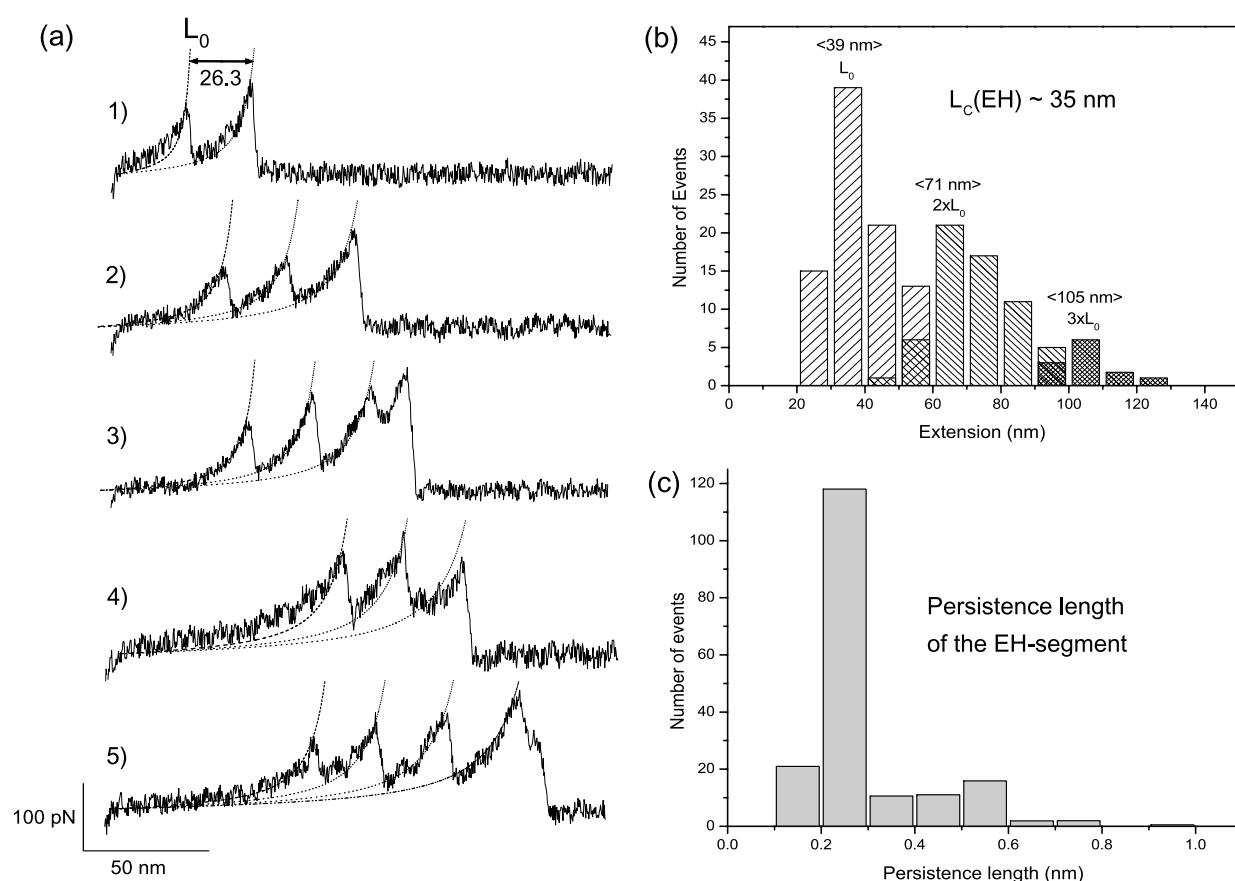


**Figure 6.** The EH-segment of myomesin has elastic properties. (a) Stretching a  $(\text{My6-EH})_4$  polyprotein with the AFM produces a saw-tooth pattern only after an initial spacer ( $\sim 20$ – $120$  nm), illustrating the elasticity contributed by the EH-domain. The saw-tooth peaks are typical for the My6 domain unfolding because they occur at around 180 pN, extend by about 26.3 nm and the recordings show one (curve 1), two (curves 2 and 4), three (curve 3), and four (curve 5) My6 unfolding events. Three discrete values of  $L_0$  can be measured, which result from stretching one (curve 1), two (curves 2 and 3) or three (curves 4 and 5) EH-segments before any My6 unfolding occurs. Pulling speed, 500 nm/s. (b) Statistical analysis of the elasticity measurements of the EH-segment. A frequency histogram of the initial length  $L_0$  shows three clearly separated peaks at 39, 71, and 105 nm. This length distribution can be explained by assuming that the initial length  $L_0$  occurs as integer multiples of about 35 nm, i.e. the contour length of the EH-segment. (c) Histogram of the persistence length distribution of the EH-domain extracted from measurements on single  $(\text{My6-EH})_4$  polyproteins showing a clear peak at  $\sim 0.3$  nm, which suggests that the EH-segment functions as an entropic spring.

the mechanical properties of EH are represented by the initial part of the force-extension curves, revealing its elastic properties. In Figure 6(b) a frequency histogram of the initial length  $L_0$  is shown. It shows three distinct peaks centered at about 39 nm, 71 nm and 105 nm. Hence, the length distribution can be explained by assuming that the initial length  $L_0$  occurs as approximately integer multiples of about 35 nm. This is consistent with the predicted contour length ( $L_C$ ) of the human EH-segment (plus linkers), which is 34.8 nm (116 aa  $\times$  0.3 nm/aa). These results suggest that the elastic properties of the initial plateau in the force-extension curves (Figure 6(a)) correspond to the extension of EH-segments of the (My6-EH)<sub>4</sub> polyprotein. The persistence length of this segment was calculated by the WLC model of polymer elasticity (Figure 6(a), dotted lines), which describes the non-linear increase in force quite accurately. A histogram of calculated persistence lengths (Figure 6(c)) shows a distribution from  $\sim 0.1$  nm to  $\sim 0.6$  nm with a clear peak at  $\sim 0.3$  nm, which is comparable to the length of one amino acid. This result indicates that the EH-segment might act as an entropic spring similar to the PEVK domain of titin.<sup>7</sup>

## Discussion

The sarcomeric cytoskeleton is responsible for ensuring the optimal interaction of the contractile filaments and proper transmission of the generated force. These functions are based largely on its remarkable elasticity, which is believed to originate from the titin filaments. We show for the first time that not only titin, but also myomesin, which was suggested to link the thick filaments in the center of the sarcomere, functions like a molecular spring. We analyzed the mechanical properties of the M-band component myomesin by AFM, TEM and CD spectroscopy. The AFM measurements of concatamers of individual myomesin domains My6 (Fn) and My10 (Ig) show a typical saw-tooth pattern in the force-extension curves, with the unfolding forces comparable with those of the Ig domains of I-band titin. The domains readily refold after relaxation. AFM measurements characterize the alternatively spliced EH-segment of myomesin as an entropic spring comparable to the PEVK domain of titin.<sup>7</sup> This characterization is complemented by TEM and CD spectroscopy, indicating that the EH-segment is a random coil with a mostly non-folded conformation.

Myomesin is a constitutive component of the sarcomeric M-band. It is expressed in all types of vertebrate striated muscle<sup>25</sup> and can be detected in the M-bands of the first sarcomeres during myofibrillogenesis.<sup>26</sup> The tight association with titin and myosin<sup>29</sup> suggests that myomesin is an integral component of the sarcomeric cytoskeleton. The myomesin molecule consists of a unique head domain, followed by 12 Fn and Ig domains. The EH-myomesin isoform contains an additional

unique segment of about 100 aa between the domains My6 and My7. This isoform, which was previously known as skelemin,<sup>43,44</sup> was originally found in embryonic heart<sup>25</sup> and later in the slow and extraocular muscle fibers of adult mice.<sup>34</sup> According to the current M-band model the neighboring myosin filaments are connected by myomesin molecules that bind with their N-terminal domains to the myosin rod<sup>28-30</sup> and dimerize in an antiparallel fashion *via* their C termini.<sup>32</sup> Considering the interaction of titin domain m4 with myomesin fragment My4-6,<sup>29</sup> myomesin in complex with titin forms the M-band filament system, which is responsible for the lateral alignment of myosin filaments. It was suggested that this system might be under tension in the activated sarcomere because the myosin filaments will try to escape from the central position due to random deviations of the cross-bridge forces on both halves.<sup>19</sup> This active mechanical role implies some structural basis for the generation of a restoring force, which counterbalances these shearing stresses.

Recent single-molecule manipulations helped to explain a potential mechanism of the restoring force generated by elastic titin filaments.<sup>4</sup> However, nothing was known until now about the mechanical properties of M-band components.

Here, we performed for the first time single-molecule measurements on myomesin. The stretching of polypeptides, constructed from the domains My6 (Fn) and My10 (Ig), resulted in a typical saw-tooth pattern demonstrating the sequential unfolding of the individual modules. The mechanical stability of the My10 (Ig) domain of myomesin is comparable with the Ig domains (I65-70) of the differentially spliced region of titin,<sup>10</sup> which is in agreement with the evolutionary relationship between these domains.<sup>45</sup> The similarity is supported by the finding that most of the Ig domains of myomesin have near their C-terminal end a glutamic (or aspartic) acid residue that is conserved in most of the Ig domains of this alternatively spliced part of titin.<sup>46</sup> In contrast to previous measurements that showed that Fn domains in titin have a mechanical stability that is in average 20% lower than the one of Ig domains,<sup>11</sup> we could not find a significant difference between the forces necessary to unfold My6 (Fn) and My10 (Ig). Since domain My6 interacts with titin<sup>29</sup> in the M-band it might participate in the formation of the M-filaments.<sup>47</sup> This is reflected by the close relation to the Fn domains of A-band titin,<sup>45</sup> which tightly associate with the thick filament. Interestingly, My6 and My10 can refold again after a relaxation phase and the folding is correct even after multiple repetitions of the stretch-release cycles, suggesting a physiological role under extreme conditions.

Some muscle types express the EH-myomesin isoform, generated by the inclusion of the EH-segment of unknown secondary structure in the center of the molecule. The analysis of the primary structure suggests that this segment has

characteristic properties, despite the rather low sequence homology between different vertebrates.<sup>25</sup> Computer simulations (PONDR) predict the EH-segment to be a disordered region with a significantly lower probability of  $\beta$ -sheet conformation. In agreement with this prediction we found that the CD spectra of the recombinant human EH-segment show the characteristics of a largely non-folded protein with residual secondary structure. Furthermore, the EH-segment is not visible in rotary shadowed specimens viewed by TEM, indicating that it is not as well folded as the Ig and Fn domains and does not form a compact structure. Interestingly, these properties of the EH-segment of myomesin are shared by the PEVK domain of titin.<sup>9,36</sup> Moreover, the AFM stretching of the (My6-EH)<sub>4</sub> polypeptide clearly shows that the EH-segment has elastic properties represented by the presence of the initial spacer equivalent to the sum of EH-segment contour lengths of 35 nm in the force-extension curves before the unfolding peaks of My6. The measured persistence length shows a clear peak at  $\sim 0.3$  nm, which is close to the theoretical value of a random coil (0.18 nm) and to the measured value of an unfolded polypeptide strand (0.4–0.8 nm<sup>8,11</sup>). The persistence length of this segment seems to be smaller compared to the PEVK domain of titin, which shows a relatively wide range of values from 0.15 nm to 2.3 nm.<sup>5,9,48,49</sup> However, it has been suggested that the PEVK region may not be a pure random coil but contains structured elements with hydrophobic interactions<sup>49</sup> and multiple elastic conformations resulting from varying degrees of proline isomerization.<sup>50</sup> This would be rather unlikely for the EH-domain because it seems to have no polyproline helices due to the smaller amount of proline residues.

By using several methods, based on different physical principles, we demonstrated that the EH-segment lacks an obvious secondary structure and functions like an entropic spring. Therefore, we propose that the EH-domain of myomesin belongs to the rapidly growing family of intrinsically unstructured/disordered proteins (IUPs).<sup>51</sup> The functional state of these proteins or protein fragments depends on the flexible, random-coil conformation under physiological conditions, which is provided by the special composition with a predominance of the so called disorder-promoting amino acids and a scarcity of order-promoting amino acids.<sup>51</sup>

In summary, EH-myomesin is a kind of miniature titin, which is also composed of stretches of Ig and Fn modules separated by largely disordered segments, the PEVK domain and the N2A or N2B sequence insertions, which are differentially expressed in heart and skeletal muscles.<sup>52,53</sup> Titin generates a restoring force based on the mechanism of entropic elasticity. In the absence of external force its entropic springs take a coiled conformation trying to maximize the entropy of its segments, while extension or compression of the chain generates a restoring force due to reduction of

entropy. The elasticity of entropic components allows titin to be extended fully reversibly at physiological forces, without the need to unfold the Ig domains.<sup>5</sup> Similar to titin, the probability for myomesin domains to unfold decreases with rising pulling speed. Thus, the domains can resist rather strong forces acting for a short time, whereas even a weak force can unfold it, being applied for a long time. Once unfolded, the domains need seconds of complete relaxation to refold. Therefore, the stability of myomesin domains is mostly endangered in the M-bands of slow twitch skeletal fibers, which are characterized by prolonged twitch duration and are active over long periods of time. Two EH-modules present in the myomesin dimer could considerably increase the elastic working range in the M-bands of slow twitch fibers and prevent the unfolding of the Fn/Ig domains of myomesin. Indeed, considering the persistence length of 0.3 nm, the end-to-end length of the EH-segment in zero-force (slack) conformation is about 6 nm, while in the fully extended state it amounts to 35 nm. The elastic force might rapidly align the thick filaments during relaxation, while the refolding of Fn and Ig modules might be not completed before the next contraction in constantly active muscles. Although the significance of this is not completely clear at the moment, the expression of myomesin isoforms seems to correlate with the expression of titin isoforms at least in some muscle types. Indeed, the developmental control of titin isoform expression leads to a shift from longer isoforms in the fetal heart to shorter isoforms in the adult heart,<sup>54,55</sup> similar to the predominant expression of the EH-isoform in the embryonic heart compared to a predominance of myomesin lacking the EH-segment in adult heart. The expression of longer titin isoforms in soleus muscle<sup>56</sup> also correlates with the presence of EH-myomesin there.<sup>34</sup> This coordinated regulation of the M-band protein composition, as well as the titin isoform content, probably reflects adaptations of the sarcomeric cytoskeleton to the special functional regime in different muscles.

We suggest that myomesin is a molecular spring characterized by complex visco-elastic properties and propose a mechanical portrait for this protein, which describes the behavior of myomesin under stretch (Figure 7). The elastic component arises from the extension of the serially linked Fn/Ig domains chain and the alternatively spliced EH-segment. These behave as two entropic springs with different stiffness in a similar way to the tandem Ig segments and the PEVK domain of titin.<sup>6</sup> In the relaxed muscle, the myomesin dimers are in a compact state. During sarcomere activation the myomesin molecules may be straightened due to small misalignments of the neighboring myosin filaments. The compliant Fn/Ig domains chain will be stretched first, followed by the extension of the stiffer EH-segment. The additional elasticity brought in by the EH-segment seems to be correlated to the working length range of

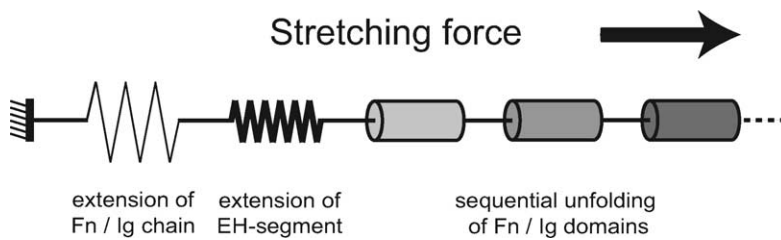


**Figure 7.** Myomesin is a molecular spring: in the relaxed state it is in a coiled conformation. Its behavior during extension might be modelled as series of elastic springs with different stiffness together with the viscous elements, corresponding to the unfolding of individual domains. Stretch would

result first in the straightening of the Fn/Ig domains chain, followed by the extension of the stiffer EH-segment. The tightly folded Fn and Ig domains might function as “shock absorbers” by reversible unfolding only in the case of extremely high or extremely long stretching forces. This mechanism might prevent the permanent rupture of the M-band filaments due to overstretching in the process of sarcomere contraction.

sarcomeres<sup>19</sup> and may help to prevent the opening of Fn/Ig modules, which need a rather long period of relaxation for refolding. However, in the case of extremely high or extremely long-lasting stretching forces the tightly folded Ig and Fn domains might function as reversible “shock absorbers” to avoid the complete rupture of the M-bands (Figure 7). These mechanical properties of the myomesin molecule are probably crucial for the stability of the sarcomeric cytoskeleton during contraction.

## Materials and Methods

### Constructing polyproteins

Polyproteins made of either identical repeats of a single myomesin domain (My6, My10) or repeats of two neighboring domains (My6-EH) were constructed using directional DNA concatemerization by self-ligation of the sticky ends of the *Ava*I restriction site.<sup>40,57</sup> Myomesin fragments with flanking *Ava*I sites were produced by PCR from the human sequence using a cDNA clone<sup>23</sup> as a template. This restriction site was used since it is asymmetrical, allowing directional assembly of the monomers. The repeats were connected by a Leu-Gly linker, corresponding to the translation of codons of the *Ava*I site. The ligation products were transformed into the recombination-defective *Escherichia coli* strain SURE 2 (Stratagene, Milano, Italy) and the colonies were analyzed directly by restriction digestion. A modified pET vector (pET*Ava*I)<sup>58</sup> was used for expression in the *E. coli* strain BLR(DE3) (Novagene, Heidelberg, Germany), consisting of a His-tag at the N terminus, a unique CTCGGG *Ava*I cloning site (verified by sequencing), and two cysteine residues on the C terminus (for covalent attachment to gold-coated coverslips). The bacteria were lysed using lysozyme (1 mg/ml) and the proteins were purified by Ni<sup>2+</sup> affinity chromatography (Protino Ni 2000; Macherey-Nagel AG, Oensingen, Switzerland). The purified polyproteins were dialyzed to PBS buffer (137 mM sodium chloride, 6.5 mM sodium phosphate, 2.7 mM potassium chloride, 1.5 mM potassium phosphate, pH 7.4) and the purity and integrity was monitored by SDS-polyacrylamide gel electrophoresis (SDS-PAGE).<sup>25</sup> Then the proteins were kept in PBS containing 5 mM DTT at 4 °C or –20 °C.

### Expression of recombinant EH-segment of myomesin

The human EH-segment was amplified by PCR from EST clone (AA248352) and subcloned into the *Bgl*III and

*Eco*RI sites of pGEX-2T (Amersham Biosciences Europe GmbH, Freiburg, Germany). It was expressed in the *E. coli* strain BL-21(DE3)star (Novagene, Heidelberg, Germany) as a glutathione S-transferase fusion protein and was purified from crude bacterial lysates by affinity chromatography on glutathione-agarose (Amersham Biosciences Europe GmbH, Freiburg, Germany) and by thrombin (isolated from human plasma, T-6884; Sigma, Buchs, Switzerland) digestion. The recombinant EH-segment was dialyzed to PBS buffer and the purity and integrity was monitored by SDS-PAGE. Then the protein was kept at –20 °C.

### Electron microscopy

After dialysis against PBS, the purified polyproteins were either kept on ice or snap-frozen in liquid nitrogen and kept at 20 °C. Immediately before spraying the samples onto a piece of freshly cleaved mica, glycerol was added to a final concentration of 30% (v/v). Sprayed samples were dried in an evaporator and then rotary shadowed at a low elevation angle (3–5°) with platinum/carbon. Micrographs were recorded on a Hitachi H-7000 transmission electron microscope (Hitachi Ltd., Tokyo, Japan) operated at 100 kV. For preparing Figures, micrographs were digitized with a scanner (HP Scan Jet IICx) at a step size of 600 dpi. The digitized micrographs were processed using Adobe Photoshop CS 8.0 software (Adobe Systems Inc., Mountain View, CA).

### Atomic force microscopy

Protein samples (50 µl, at a concentration of 5–50 µg/ml) were deposited onto freshly coated gold or glass coverslips and allowed to adsorb onto the surface for 2–20 minutes before washing away unbound protein with excess buffer.<sup>9</sup> Force-extension measurements were then carried out in PBS buffer at pulling speeds from 125 nm/s to 4000 nm/s. The force transducer was a standard silicon nitride micro cantilever (OMCL-Bio-Lever) from Olympus (with a typical spring constant of 6 pN/nm), whose stiffness was calibrated *in situ* in solution for each separate experiment as described by Hutter.<sup>59</sup> Saw-tooth data were acquired, and the peak forces were recorded using LabView 6.1 (National Instruments, Austin, TX). Representation and curve fitting of the data were done using Origin 7.0 (OriginLab Corporation, Northampton, MA).

### Circular dichroism spectroscopy

Circular dichroic experiments were performed at room temperature using a Jasco J-810 spectropolarimeter. The

far-CD spectrum was recorded from 190 nm to 250 nm with quartz cells of 1 mm path length. After dialyzing to PBS, the protein concentration was determined by the absorbance coefficient at 280 nm. The purified EH-segment was diluted to 20  $\mu$ M in PBS for obtaining the CD spectrum, which was corrected by subtracting the buffer baseline.

### Sequence analysis

The boundaries of domains My6 and My10 of human myomesin were determined on the basis of crystal structures of the nearest neighbors, predicted by ncbi (conserved domain database). These were an Fn domain of the cytokine-binding region of human Gp130 (for My6) and an Ig domain of the mouse immunoglobulin Fab fragment (heavy chain, for My10). According to this structural analysis, the My6 domain has 88 aa residues and a linker length of 15 residues. The My10 domain spans 95 aa with 35 aa long linkers between the domains. The EH-segment has a length of 96 aa (116 aa including natural linkers in the polypeptide). Protein disorder analysis of myomesin was performed using PONDR<sup>®</sup> (Predictors of Natural Disordered Regions). Access to PONDR<sup>®</sup> was provided by Molecular Kinetics (6201 La Pas Trail - Ste 160, Indianapolis, IN 46268; 317-280-8737; E-mail: [main@molecularkinetics.com](mailto:main@molecularkinetics.com)). VL-XT is copyright©1999 by the WSU Research Foundation, all rights reserved. PONDR<sup>®</sup> is copyright©2004 by Molecular Kinetics, all rights reserved.

### Acknowledgements

We are grateful to Dr Mariano Carrion-Vazquez and Dr Julio M. Fernandez for the generous donation of the pETAval vector and for advice. We thank Dr Eva Kuennemann and Professor Rudolf Glockshuber for helping with the CD spectroscopy measurements. In addition, we thank Stephan Lange for technical help and Dr Elisabeth Ehler for stimulating discussions and critical reading of the manuscript. Furthermore, we thank Professor Wolfgang Linke for great advice. P.B. was supported by a research grant from Roche (Grant Mkl/stm 206-2003). M.H. was funded by the EUCOR Learning Teaching Mobility "Nanoscience" project. G.M. and U.A. acknowledge the support of the M.E. Müller Foundation and the Canton Basel-Stadt. In addition, this work was funded by grants from the SNF (M.H. & J.C.P.), the Swiss Foundation on Research of Muscle Diseases and by the SUK Grant to the Swiss Cardiovascular Teaching and Research Network. R.S. was supported by a predoctoral training grant from ETH.

### References

- Trinick, J., Knight, P. & Whiting, A. (1984). Purification and properties of native titin. *J. Mol. Biol.* **180**, 331–356.
- Fürst, D. O., Osborn, M., Nave, R. & Weber, K. (1988). The organization of titin filaments in the half-sarcomere revealed by monoclonal antibodies in immunoelectron microscopy: a map of ten non-repetitive epitopes starting at the Z line extends close to the M line. *J. Cell Biol.* **106**, 1563–1572.
- Tskhovrebova, L. & Trinick, J. (2003). Titin: properties and family relationships. *Nature Rev. Mol. Cell Biol.* **4**, 679–689.
- Granzier, H. L. & Labeit, S. (2004). The giant protein titin: a major player in myocardial mechanics, signaling, and disease. *Circ. Res.* **94**, 284–295.
- Tskhovrebova, L., Trinick, J., Sleep, J. A. & Simmons, R. M. (1997). Elasticity and unfolding of single molecules of the giant muscle protein titin. *Nature*, **387**, 308–312.
- Trombitas, K., Greaser, M., Labeit, S., Jin, J. P., Kellermayer, M., Helmes, M. & Granzier, H. (1998). Titin extensibility in situ: entropic elasticity of permanently folded and permanently unfolded molecular segments. *J. Cell Biol.* **140**, 853–859.
- Linke, W. A., Kulke, M., Li, H., Fujita-Becker, S., Neagoe, C., Manstein, D. J. *et al.* (2002). PEVK domain of titin: an entropic spring with actin-binding properties. *J. Struct. Biol.* **137**, 194–205.
- Rief, M., Gautel, M., Oesterhelt, F., Fernandez, J. M. & Gaub, H. E. (1997). Reversible unfolding of individual titin immunoglobulin domains by AFM. *Science*, **276**, 1109–1112.
- Li, H., Linke, W. A., Oberhauser, A. F., Carrion-Vazquez, M., Kerkvliet, J. G., Lu, H. *et al.* (2002). Reverse engineering of the giant muscle protein titin. *Nature*, **418**, 998–1002.
- Watanabe, K., Muhle-Goll, C., Kellermayer, M. S., Labeit, S. & Granzier, H. (2002). Different molecular mechanics displayed by titin's constitutively and differentially expressed tandem Ig segments. *J. Struct. Biol.* **137**, 248–258.
- Rief, M., Gautel, M., Schemmel, A. & Gaub, H. E. (1998). The mechanical stability of immunoglobulin and fibronectin III domains in the muscle protein titin measured by atomic force microscopy. *Biophys. J.* **75**, 3008–3014.
- Tskhovrebova, L. & Trinick, J. (2004). Properties of titin immunoglobulin and fibronectin-3 domains. *J. Biol. Chem.* **279**, 46351–46354.
- Kellermayer, M. S., Smith, S. B., Bustamante, C. & Granzier, H. L. (1998). Complete unfolding of the titin molecule under external force. *J. Struct. Biol.* **122**, 197–205.
- Page, S. G. & Huxley, H. E. (1963). Filament lengths in striated muscle. *J. Cell Biol.* **19**, 369–390.
- Bergman, R. A. (1983). Ultrastructural configuration of sarcomeres in passive and contracted frog sartorius muscle. *Am. J. Anat.* **166**, 209–222.
- Horowitz, R. & Podolsky, R. J. (1987). The positional stability of thick filaments in activated skeletal muscle depends on sarcomere length: evidence for the role of titin filaments. *J. Cell Biol.* **105**, 2217–2223.
- Horowitz, R. & Podolsky, R. J. (1988). Thick filament movement and isometric tension in activated skeletal muscle. *Biophys. J.* **54**, 165–171.
- Horowitz, R., Maruyama, K. & Podolsky, R. J. (1989). Elastic behavior of connectin filaments during thick filament movement in activated skeletal muscle. *J. Cell Biol.* **109**, 2169–2176.
- Agarkova, I., Ehler, E., Lange, S., Schoenauer, R. & Perriard, J. C. (2003). M-band: a safeguard for sarcomere stability? *J. Muscle Res. Cell Motil.* **24**, 191–203.
- Obermann, W. M. J., Gautel, M., Steiner, F., Vanderven, P. F. M., Weber, K. & Fürst, D. O. (1996).

- The structure of the sarcomeric M band: localization of defined domains of myomesin, M-protein, and the 250-kD carboxy-terminal region of titin by immunoelectron microscopy. *J. Cell Biol.* **134**, 1441–1453.
21. Nave, R., Fürst, D. O. & Weber, K. (1989). Visualization of the polarity of isolated titin molecules: a single globular head on a long thin rod as the M band anchoring domain? *J. Cell Biol.* **109**, 2177–2187.
  22. Bantle, S., Keller, S., Haussmann, I., Auerbach, D., Perriard, E., Mühlebach, S. & Perriard, J. C. (1996). Tissue-specific isoforms of chicken myomesin are generated by alternative splicing. *J. Biol. Chem.* **271**, 19042–19052.
  23. Vinkemeier, U., Obermann, W., Weber, K. & Fürst, D. O. (1993). The globular head domain of titin extends into the center of the sarcomeric M band. cDNA cloning, epitope mapping and immunoelectron microscopy of two titin-associated proteins. *J. Cell Sci.* **106**, 319–330.
  24. Grove, B. K., Holmbom, B. & Thornell, L. E. (1987). Myomesin and M protein: differential expression in embryonic fibers during pectoral muscle development. *Differentiation*, **34**, 106–114.
  25. Agarkova, I., Auerbach, D., Ehler, E. & Perriard, J. C. (2000). A novel marker for vertebrate embryonic heart, the EH-myomesin isoform. *J. Biol. Chem.* **275**, 10256–10264.
  26. Ehler, E., Rothen, B. M., Hämmerle, S. P., Komiyama, M. & Perriard, J. C. (1999). Myofibrillogenesis in the developing chicken heart: assembly of Z-disk, M-line and the thick filaments. *J. Cell Sci.* **112**, 1529–1539.
  27. Gotthardt, M., Hammer, R. E., Hubner, N., Monti, J., Witt, C. C., McNabb, M. *et al.* (2003). Conditional expression of mutant M-line titins results in cardiomyopathy with altered sarcomere structure. *J. Biol. Chem.* **278**, 6059–6065.
  28. Obermann, W. M., Plessmann, U., Weber, K. & Fürst, D. O. (1995). Purification and biochemical characterization of myomesin, a myosin-binding and titin-binding protein, from bovine skeletal muscle. *Eur. J. Biochem.* **233**, 110–115.
  29. Obermann, W. M. J., Gautel, M., Weber, K. & Fürst, D. O. (1997). Molecular structure of the sarcomeric M band: mapping of titin and myosin binding domains in myomesin and the identification of a potential regulatory phosphorylation site in myomesin. *EMBO J.* **16**, 211–220.
  30. Auerbach, D., Bantle, S., Keller, S., Hinderling, V., Leu, M., Ehler, E. & Perriard, J. C. (1999). Different domains of the M-band protein myomesin are involved in myosin binding and M-band targeting. *Mol. Biol. Cell*, **10**, 1297–1308.
  31. Hornemann, T., Kempa, S., Himmel, M., Hayess, K., Fürst, D. O. & Wallimann, T. (2003). Muscle-type creatine kinase interacts with central domains of the M-band proteins myomesin and M-protein. *J. Mol. Biol.* **332**, 877–887.
  32. Lange, S., Himmel, M., Auerbach, D., Agarkova, I., Hayess, K., Fürst, D. O. *et al.* (2005). Dimerisation of myomesin: implications for the structure of the sarcomeric M-band. *J. Mol. Biol.* **345**, 289–298.
  33. Steiner, F., Weber, K. & Fürst, D. O. (1999). M-band proteins myomesin and skelemin are encoded by the same gene: analysis of its organization and expression. *Genomics*, **56**, 78–89.
  34. Agarkova, I., Schoenauer, R., Ehler, E., Carlsson, L., Carlsson, E., Thornell, L. E. & Perriard, J. C. (2004). The molecular composition of the sarcomeric M-band correlates with muscle fiber type. *Eur. J. Cell Biol.* **83**, 193–204.
  35. Kellermayer, M. S., Smith, S. B., Granzier, H. L. & Bustamante, C. (1997). Folding-unfolding transitions in single titin molecules characterized with laser tweezers. *Science*, **276**, 1112–1116.
  36. Ma, K. & Wang, K. (2003). Malleable conformation of the elastic PEVK segment of titin: non-co-operative interconversion of polyproline II helix, beta-turn and unordered structures. *Biochem. J.* **374**, 687–695.
  37. Oberhauser, A. F., Badilla-Fernandez, C., Carrion-Vazquez, M. & Fernandez, J. M. (2002). The mechanical hierarchies of fibronectin observed with single-molecule AFM. *J. Mol. Biol.* **319**, 433–447.
  38. Bouchiat, C., Wang, M. D., Allemand, J., Strick, T., Block, S. M. & Croquette, V. (1999). Estimating the persistence length of a worm-like chain molecule from force-extension measurements. *Biophys. J.* **76**, 409–413.
  39. Zhang, B. & Evans, J. S. (2001). Modeling AFM-induced PEVK extension and the reversible unfolding of Ig/FNIII domains in single and multiple titin molecules. *Biophys. J.* **80**, 597–605.
  40. Carrion-Vazquez, M., Marszalek, P. E., Oberhauser, A. F. & Fernandez, J. M. (1999). Atomic force microscopy captures length phenotypes in single proteins. *Proc. Natl Acad. Sci. USA*, **96**, 11288–11292.
  41. Politou, A. S., Thomas, D. J. & Pastore, A. (1995). The folding and stability of titin immunoglobulin-like modules, with implications for the mechanism of elasticity. *Biophys. J.* **69**, 2601–2610.
  42. Soteriou, A., Clarke, A., Martin, S. & Trinick, J. (1993). Titin folding energy and elasticity. *Proc. R. Soc. London B. Biol. Sci.* **254**, 83–86.
  43. Price, M. G. (1987). Skelemins: cytoskeletal proteins located at the periphery of M-discs in mammalian striated muscle. *J. Cell Biol.* **104**, 1325–1336.
  44. Price, M. G. & Gomer, R. H. (1993). Skelemin, a cytoskeletal M-disc periphery protein, contains motifs of adhesion/recognition and intermediate filament proteins. *J. Biol. Chem.* **268**, 21800–21810.
  45. Kenny, P. A., Liston, E. M. & Higgins, D. G. (1999). Molecular evolution of immunoglobulin and fibronectin domains in titin and related muscle proteins. *Gene*, **232**, 11–23.
  46. Witt, C. C., Olivieri, N., Centner, T., Kolmerer, B., Millevoi, S., Morell, J. *et al.* (1998). A survey of the primary structure and the interspecies conservation of I-band titin's elastic elements in vertebrates. *J. Struct. Biol.* **122**, 206–215.
  47. Luther, P. & Squire, J. (1978). Three-dimensional structure of the vertebrate muscle M-region. *J. Mol. Biol.* **125**, 313–324.
  48. Watanabe, K., Nair, P., Labeit, D., Kellermayer, M. S., Greaser, M., Labeit, S. & Granzier, H. (2002). Molecular mechanics of cardiac titin's PEVK and N2B spring elements. *J. Biol. Chem.* **277**, 11549–11558.
  49. Leake, M. C., Wilson, D., Gautel, M. & Simmons, R. M. (2004). The elasticity of single titin molecules using a two-bead optical tweezers assay. *Biophys. J.* **87**, 1112–1135.
  50. Li, H., Oberhauser, A. F., Redick, S. D., Carrion-Vazquez, M., Erickson, H. P. & Fernandez, J. M. (2001). Multiple conformations of PEVK proteins detected by single-molecule techniques. *Proc. Natl Acad. Sci. USA*, **98**, 10682–10686.
  51. Tompa, P. (2002). Intrinsically unstructured proteins. *Trends Biochem. Sci.* **27**, 527–533.

52. Labeit, S. & Kolmerer, B. (1995). Titins: giant proteins in charge of muscle ultrastructure and elasticity. *Science*, **270**, 293–296.
53. Trombitas, K., Freiburg, A., Centner, T., Labeit, S. & Granzier, H. (1999). Molecular dissection of N2B cardiac titin's extensibility. *Biophys. J.* **77**, 3189–3196.
54. Lahmers, S., Wu, Y., Call, D. R., Labeit, S. & Granzier, H. (2004). Developmental control of titin isoform expression and passive stiffness in fetal and neonatal myocardium. *Circ. Res.* **94**, 505–513.
55. Opitz, C. A., Leake, M. C., Makarenko, I., Benes, V. & Linke, W. A. (2004). Developmentally regulated switching of titin size alters myofibrillar stiffness in the perinatal heart. *Circ. Res.* **94**, 967–975.
56. Freiburg, A., Trombitas, K., Hell, W., Cazorla, O., Fougousse, F., Centner, T. *et al.* (2000). Series of exon-skipping events in the elastic spring region of titin as the structural basis for myofibrillar elastic diversity. *Circ. Res.* **86**, 1114–1121.
57. Hartley, J. L. & Gregori, T. J. (1981). Cloning multiple copies of a DNA segment. *Gene*, **13**, 347–353.
58. Carrion-Vazquez, M., Oberhauser, A. F., Fisher, T. E., Marszalek, P. E., Li, H. & Fernandez, J. M. (2000). Mechanical design of proteins studied by single-molecule force spectroscopy and protein engineering. *Prog. Biophys. Mol. Biol.* **74**, 63–91.
59. Hutter, J. L. & Bechhoefer, J. (1993). Calibration of atomic-force microscope tips. *Rev. Sci. Instrum.* **64**, 1868–1873.

*Edited by J. Karn*

*(Received 31 January 2005; received in revised form 11 March 2005; accepted 21 March 2005)*